Journal of Electronic Materials (2024) 53:6282–6289
https://doi.org/10.1007/s11664-024-11292-6

ORIGINAL RESEARCH ARTICLE

Effect of Selenium Doping on the Electronic Properties of β-Ga_2O_3 by First-Principles Calculations

Hanzhao Song[1] · Zhigao Xie[1] · Yimin Liao[1] · Yan Wang[1] · Chee-Keong Tan[1,2,3,4]

Received: 19 February 2024 / Accepted: 25 June 2024 / Published online: 24 July 2024

Abstract

This study is the first to explore the effect of selenium doping on the electronic properties of β-Ga_2O_3 through first-principles calculations. Selenium doping in β-Ga_2O_3 is a significant choice, as it has the potential to improve the material's electronic properties. Previous work on β-Ga_2O_3 has focused primarily on other dopants, and the effect of selenium doping is not well understood. Therefore, this study fills an important gap in the current understanding of β-Ga_2O_3 doping. Selenium doping in β-Ga_2O_3 was studied by first-principles calculations with a hybrid functional, as this functional can offer a more accurate description of electronic properties, resulting in accurate electronic bandgap and defect level calculations. Our first-principles calculations reveal that selenium can be incorporated on both Ga and O sites under specific conditions. Specifically, under O-rich conditions, selenium atoms are more likely to substitute the Ga sites, whereas under Ga-rich conditions, they are more likely to substitute the O sites. With the formation energy analysis, our findings indicate that selenium doping on Ga sites can lead to n-type conductivity, with it acting as shallow donor. On the other hand, Se dopants at the O sites exhibit deep donor characteristics, rendering it ineffective in regulating the conductivity of β-Ga_2O_3 materials. Our findings suggest that Se can be used as a dopant to tune the β-Ga_2O_3 conductivity for electronic and photonic applications, provided that the atomic substitution on Ga sites can be effectively controlled. Our results will provide valuable theoretical insights for the refined use of selenium dopants in β-Ga_2O_3, as well as guidance and theoretical support for subsequent researchers in the selection of Ga_2O_3 dopants.

Keywords β-Ga_2O_3 · first-principles · defects · selenium · formation energy

Introduction

Gallium oxide (Ga_2O_3) semiconductor materials have received widespread attention for technological applications in high-power electronic devices,[1–3] deep-ultraviolet (UV) photodetectors,[4,5] and photocatalysis, among others.[6] Ga_2O_3 exists in five distinct crystalline phases: α, β, γ, δ, and ε. Among these, β-Ga_2O_3 is widely regarded as the most stable form under standard temperature and pressure conditions.[7] β-Ga_2O_3 has an ultra-wide bandgap of approximately 4.9 eV, large critical field strength of 8 MV/cm, and high optical transmittance in the deep-ultraviolet region.[8,9] Additionally, it boasts good chemical and thermal stability, and can be obtained at low cost in large-size, high-quality, doped bulk single crystals using the edge-defined film-fed crystal growth (EFG) method.[10] With the improvement in epitaxial techniques and computational methods, recent work has also been extended to Ga_2O_3 alloying including BGaO, InGaO, and AlGaO.[11–15] However, the drawbacks in Ga_2O_3 alloys,

✉ Chee-Keong Tan
cheekeongtan@hkust-gz.edu.cn

1 Advanced Materials Thrust, Function Hub, The Hong Kong University of Science and Technology (Guangzhou), Nansha, Guangzhou 511466, China

2 Department of Electronic and Computer Engineering, Hong Kong University of Science and Technology, Hong Kong, China

3 Guangzhou Municipal Key Laboratory of Materials Informatics, The Hong Kong University of Science and Technology (Guangzhou), Guangzhou 511453, Guangdong, China

4 Guangzhou Municipal Key Laboratory of Integrated Circuits Design, The Hong Kong University of Science and Technology (Guangzhou), Guangzhou 511453, Guangdong, China

specifically the low thermal conductivity, challenges with p-type doping, and inadequate conductivity,[16] have impeded its further development in recent years.

The conductivity of intrinsic β-Ga_2O_3 materials can be achieved by doping Ga_2O_3 materials with other elements. Among n-type dopants, Si, Ge, Sn, Cl, and F have been found to be shallow donors, and hydrogen impurities have been discovered to act as donors, existing as both interstitial species and substitutional donors on oxygen sites, but their effectiveness in achieving the desired conductivity levels in β-Ga_2O_3 is limited.[17–20] Peelaers and Van de Walle[21] found that W, Mo, and Re were deep donors, and the presence of these deep donor dopants further complicates the control of conductivity in β-Ga_2O_3. Among p-type dopants, Lyons[22] found that the introduction of Be, Mg, Ca, Sr, Zn, Cd, and N through doping is likely to induce p-type conductivity. However, the acceptor transition levels of these dopants were found to be higher than 1.3 eV, making them ineffective in creating the free holes necessary for p-type conductivity. The limitations of traditional dopants and the challenge of achieving desired conductivity levels in β-Ga_2O_3 materials necessitate the exploration of alternative dopants and new methods to enhance the electronic properties of β-Ga_2O_3. This has prompted the investigation of a wide range of elements, such as metal elements Cu,[23] Fe,[24] Cr,[25] Mn,[26] and Nb,[27] and rare earth elements Eu,[28] Tb,[29] Tm,[30] and Er.[31] Selenium dopants are potentially good candidates, as they share the same group with O in the periodic table, which allows for effective incorporation into the crystal lattice and facilitates the control and manipulation of the electronic properties of the materials. The exploration of selenium as a dopant for β-Ga_2O_3 is a promising new approach for addressing the limitations of traditional dopants and has the potential to provide solutions to challenges associated with controlling β-Ga_2O_3 conductivity. Therefore, the investigation of selenium doping in β-Ga_2O_3 through first-principles calculations is a significant step in advancing the understanding of alternative dopants and their potential to improve the electronic properties of β-Ga_2O_3. Selenium as a dopant has yet to be explored for β-Ga_2O_3, despite the theoretical and experimental studies on GaOSe alloying.[32,33] Thus, it is important to investigate the selenium doping effect on the electronic properties of β-Ga_2O_3, with the aim of finding the remedy for controlling n-type and p-type conductivity of β-Ga_2O_3. However, the process of experimentally studying this issue can be complex and time-consuming. Therefore, first-principles calculations were chosen for this research due to their ability to provide accurate and reliable predictions of material properties and behaviors at the atomic and electronic levels without the need for experimental data or fitting parameters.

In this study, we investigated the impact of selenium doping on the electronic properties of β-Ga_2O_3 through first-principles calculations with a novel hybrid functional. We specifically focused on investigating the preferred doping sites for selenium in different environments, examining the formation energies and charge transition levels of selenium dopants in β-Ga_2O_3, and analyzing the density of states of Se-doped β-Ga_2O_3 to understand their effect on conductivity and electronic properties. In the following sections, we will thoroughly explore the methods employed in our research and the resulting outcomes. This comprehensive analysis will provide a deeper understanding of our study and its implications. The findings of our work offer valuable insights and theoretical support for selenium doping in β-Ga_2O_3, providing useful guidance in this area.

Method

All calculations were carried out using the Vienna Ab initio Simulation Package (VASP),[34] which is based on density functional theory (DFT) and utilizes the projector-augmented plane wave (PAW) pseudopotential method.[35,36] After convergence tests, the cutoff energy was set at 520 eV, with the force on each atom kept below 0.01 eV/Å and the total energy convergence reaching 1×10^{-5} eV/atom. All the above technical parameters were verified by convergence tests. The Perdew–Burke–Ernzerhof generalized gradient approximation (GGA-PBE) functional was employed to perform structural optimization due to its accurate description of exchange–correlation energy in various materials and good performance in predicting lattice constants, bond lengths, and angles, making it reliable for structural optimization.[37] The HSE06 hybrid functional, with a mixing parameter of 0.40, was chosen for band structure calculations due to its ability to accurately predict band structures and electronic properties of materials,[38] and its calculated bandgap aligns well with experimental values.[39] A 240-atom maximumly cubic supercell was generated using the Defect and Dopant ab-initio Simulation Package (DASP).[40] We considered all potential doping atomic sites and generated selenium substitution sites at non-equivalent sites based on crystal symmetry. The valence electron configurations of Se atom are $4s^2 4p^4$ and spin polarization was considered for the different defect charge states.

For example, the formation energy of Se on the O sites in charge state q in Ga_2O_3 is given by the following formula[41]:

$$\begin{aligned} E^f\left(\mathrm{Se}_\mathrm{O}^q\right) =& E_{\mathrm{tot}}\left(\mathrm{Se}_\mathrm{O}^q\right) - E_{\mathrm{tot}}\left(\mathrm{Ga_2O_3}\right) - \left(\mu_{\mathrm{Se}} + \mu_{\mathrm{Se}}^0\right) \\ &+ \left(\mu_{\mathrm{O}} + \mu_{\mathrm{O}}^0\right) + q\left(E_{\mathrm{F}} + E_{\mathrm{VBM}}\right) + \Delta^q, \end{aligned} \tag{1}$$

where $E_{\mathrm{tot}}\left(\mathrm{Se}_O^q\right)$ represents the energy of a selenium defect in charge state q in the supercell, $E_{\mathrm{tot}}\left(\mathrm{Ga_2O_3}\right)$ represents the energy of a pure Ga_2O_3 supercell, E_{F} represents the Fermi energy, measured relative to the valence band maximum (VBM), and Δ^q is the correction term.[42] In order to eliminate erroneous electrostatic interactions between

supercells containing charged defects, we utilized the Freysoldt, Neugebauer, and Van de Walle (FNV) scheme to adjust the formation energies,[43] and the details can be found in the supplementary material. μ_O and μ_{Se} are the relative chemical potential energies of the corresponding elemental materials, μ_O^0 represents the energy of an O atom within one O_2 molecule, and μ_{Se}^o is the energy of a Se atom in selenium bulk. We examined two extreme cases: O-rich ($\mu_O = 0$) and O-poor ($\mu_{Ga} = 0$) conditions. When Se is doped into Ga_2O_3, the chemical potential must satisfy three conditions: (1) the formation reaction of the target compound reaches thermodynamic equilibrium: $2\mu_{Ga} + 3\mu_O = \Delta H_f(Ga_2O_3)$, (2) the simple substances of the constituent elements of the host compound will not form: $\mu_{Ga} < 0$, $\mu_O < 0$, and (3) the formation of competing secondary compounds related to the host compound cannot occur: $\mu_{Se} < 0$, $\mu_{Ga} + \mu_{Se} < \Delta H_f(GaSe)$. Here, both Se and GaSe crystals were identified as key impurity phases for Se doping in Ga_2O_3.[40] The charge-state transition $\varepsilon(q_1/q_2)$ can be obtained by the following formula[41]:

$$\varepsilon(q_1/q_2) = \frac{E^f(X^{q_1};E_F = 0) - E^f(X^{q_2};E_F = 0)}{q_2 - q_1}. \quad (2)$$

Results and Discussion

Crystal Structure and Band Structure

Figure 1 shows the crystal structure of a conventional β-Ga_2O_3 cell. β-Ga_2O_3 crystal has a monoclinic structure with space group C2/m. There are two types of Ga atom sites and three types of O atom sites in the β-Ga_2O_3 conventional cell, as labeled in Fig. 1. Half of the Ga atoms are tetrahedrally coordinated as Ga(I), while the other half are octahedrally coordinated as Ga(II). Both O(I) and O(II) are threefold-coordinated, while O(III) is fourfold-coordinated. O(I) is positioned at the shared corner of one GaO_4 tetrahedron and two GaO_6 octahedra, while O(II) is located at the shared corner of one GaO_6 octahedron and two GaO_4 tetrahedra. The calculated structural parameters and bandgap of β-Ga_2O_3 are shown in Table I. These structural parameter values are in agreement with the experimental results[44] and those reported by Liu et al.[32]

Figure 2 illustrates the band structure of the primitive cell of β-Ga_2O_3, which was calculated using the HSE06 functional with a mixing parameter of 0.40. It can be observed that the conduction band minimum (CBM) is positioned at the Γ-point, whereas the valence band maximum (VBM) is situated at the I-L line. The measured direct energy bandgap of 4.93 eV aligns well with the experimental values[45] and those reported by Liu et al.[32] Moreover, the direct gap at the Γ-point is slightly larger, measuring 4.93 eV.

Defect Formation Energy and Transition Level

Figure 3a shows the model of the undoped β-Ga_2O_3 supercell, while Fig. 3b, c, d, e, and f show the Se-doped β-Ga_2O_3 model with substitutional Se on the Ga(I), Ga(II), O(I), O(II), and O(III) sites, respectively. All structural models are the 240-atom maximumly cubic supercell generated using the software package (DASP).[40] It can be clearly seen that all the models have two nonequivalent Ga atoms and

Table I Calculated structural parameters and bandgap of β-Ga_2O_3

Parameter	This work	Experiment	Ref. [32]
a (Å)	12.47	12.23 ± 0.02[a]	12.26
b (Å)	3.09	3.04 ± 0.01[a]	5.76
c (Å)	5.88	5.80 ± 0.01[a]	5.82
β (°)	103.68	103.7 ± 0.3[a]	–
$E_{gap}^{indirect}$(eV)	4.90	–	4.835
E_{gap}^{direct}(eV)	4.93	4.76[b]	4.868

[a]Ref. [44], [b]Ref. [45].

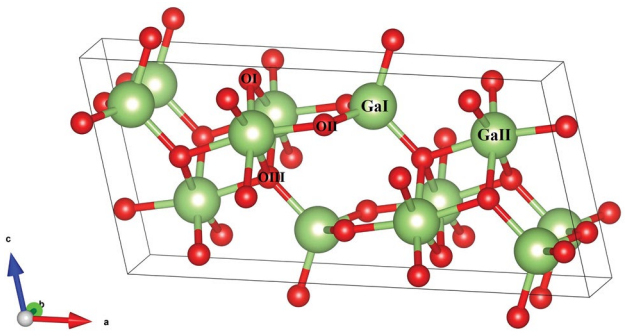

Fig. 1 Crystal structure of β-Ga_2O_3 conventional cell.

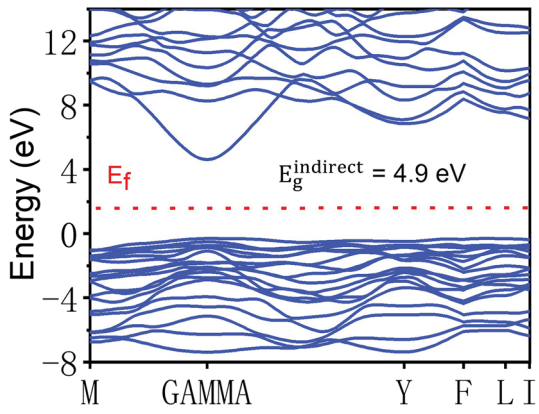

Fig. 2 Calculated band structure of β-Ga_2O_3 primitive cell.

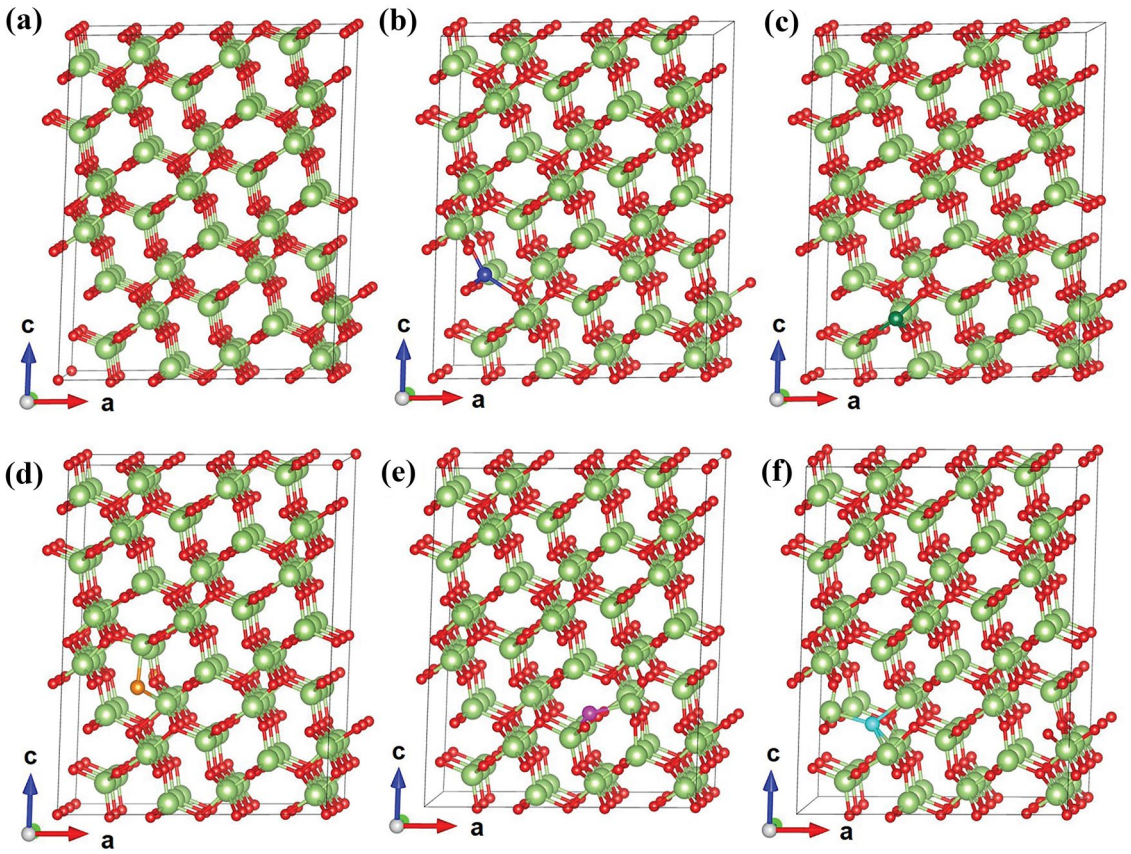

Fig. 3 The model diagrams of the β-Ga_2O_3 supercell: (a) undoped, (b) Ga(I), (c) Ga(II), (d) O(I), (e) O(II), and (f) O(III) Se-doped sites.

three nonequivalent O atoms. The different doping models are generated by the substitution of one Se atom at different sites.

As illustrated in Fig. 4a, under gallium-rich conditions, the formation energy of selenium on oxygen sites is lower than that on gallium sites, indicating a higher likelihood of selenium substituting the oxygen sites. Conversely, in Fig. 4b, under oxygen-rich conditions, the formation energy of selenium on gallium sites is lower, implying a greater chance for selenium atoms to substitute gallium sites. Additionally, in its neutral charge state, the formation energy of selenium on the O(I) sites is lower than on other oxygen sites, making it more stable. The preference for selenium to substitute oxygen sites under gallium-rich conditions can be attributed to the higher concentration of gallium vacancies or other defects that create a favorable environment for selenium to occupy oxygen sites. Conversely, under oxygen-rich conditions, the excess of oxygen atoms may lead to a greater likelihood for selenium to substitute gallium sites, as the availability of gallium vacancies or other defects becomes more prominent. The stability of selenium on O(I) sites in its neutral charge state further emphasizes the preferential substitution of selenium on these specific oxygen sites. This preference can be attributed to the local chemical environment and electronic structure of the O(I) sites, which may offer a more energetically favorable configuration for selenium incorporation. The implications of these substitution preferences extend to the electronic properties of β-Ga_2O_3. The specific doping configurations of selenium on different sites can significantly influence the material's electronic band structure, charge carrier mobility, and optical properties. Our initial investigation focused on the incorporation of selenium on gallium sites in Ga_2O_3. Selenium atoms have two 4*s* electrons and four 4*p* electrons, while gallium has two 4*s* electrons and one 4*p* electron. By substituting selenium on a gallium site, three additional electrons are introduced, turning selenium into a potential triple donor. The different bonding environments of the two nonequivalent gallium sites can result in varying formation energies and charge-state transition levels.[21] As shown in Fig. 4c, the transition level of (0/+) is 4.848 eV on Ga(I) sites and is 4.833 eV on Ga(II) sites, indicating that it is easy to donate an electron to the conduction band with high Fermi levels in the bandgap for 1+ charge states. Thus, Se on the Ga sites also acts as a shallow donor. However, the 3+ charge states are stable when Fermi levels in the bandgap are lower. Selenium

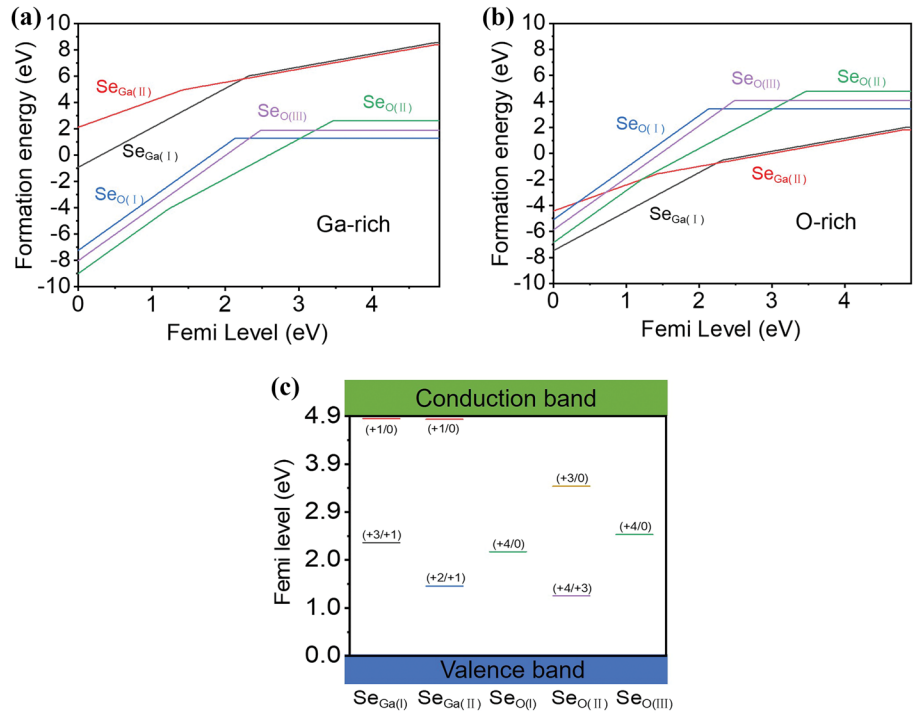

Fig. 4 Formation energy diagram of Se on Ga or O sites for (a) Ga-rich, (b) O-rich, (c) transition levels of Se doping in β-Ga_2O_3.

doping in β-Ga_2O_3 has been found to be an effective n-type dopant, leading to improved electrical conductivity in the materials. In comparison to other n-type dopants such as silicon, selenium doping has been shown to be equally effective. Next, we consider Se incorporation on O sites in Ga_2O_3. The Se atom is in the same main group as the O atom and has the same number of valence electrons. So, when a Se atom substitutes the O atom, it is still basically electrically neutral. However, due to the difference in atomic number, electronegativity, and covalent radius between the O atom and Se atom, when a Se atom substitutes the O atom, it can capture a certain carrier to become a charged center called an isoelectronic trap.[46] The radius of the Se atom is larger than that of the O atom, and the electronegativity of the O and Se atoms is 3.44 and 2.48, respectively. For the O(I) site, the transition levels of (0/+), (0/2+), (0/3+), and (0/4+) are 1.938 eV, 1.762 eV, 2.037 eV, and 2.13 eV, respectively. Likewise, for the O(II) site, the transition levels are 2.766 eV, 2.787 eV, 3.466 eV, and 2.906 eV, and for the O(III) site, they are 2.101 eV, 1.887 eV, 1.591 eV, and 2.482 eV, respectively. This energy level has no effect on the type of conductivity. Thus, selenium doping can impact the performance of high-power devices by fine-tuning the conductivity of β-Ga_2O_3. This can lead to improved electrical properties, higher breakdown voltage, enhanced power handling capability, and better thermal management, ultimately contributing to the development of more efficient and reliable high-power electronic devices.

Density of States

As depicted in Fig. 5a, the projected density of states (PDOS) illustrates that the band edges of pure β-Ga_2O_3 are dominated by O 2*p* and Ga 4*s* orbitals. The bandgap of β-Ga_2O_3 is determined by the occupancy of the valence band maximum (VBM) by O 2*p* orbital electrons and the conduction band minimum (CBM) by Ga 4*s* orbital electrons. Figure 5b, c, d, e, and f shows the projected density of states of Se-doped β-Ga_2O_3 at different sites. The figure reveals that the PDOS (partial density of states) for Ga and O exhibits minimal changes following doping. Consequently, our focus primarily lies on the contribution of impurity elements to the density of states. Upon Se doping at Ga sites, we observed a slight decrease in the bandgap. This can be attributed to the presence of Se as shallow donor impurities, causing the energy states of Se impurities to expand and overlap with the conduction band. On the other hand, the occupation of the VB edge by the O 2*p* orbital is mildly influenced by Se doping, which was previously suggested by Liu and co-worker.[32] In general, the doping of Se possibly leads to orbital hybridization in both valence and conduction bands of Ga_2O_3.

First-principles calculations offer valuable forecasts for selenium doping in β-Ga_2O_3, but they need simplifications in modeling electronic interactions, which limit the accuracy of the results.

Thus, integrating these computational findings with experimental data can help provide a more comprehensive understanding of the impact of selenium doping on the properties

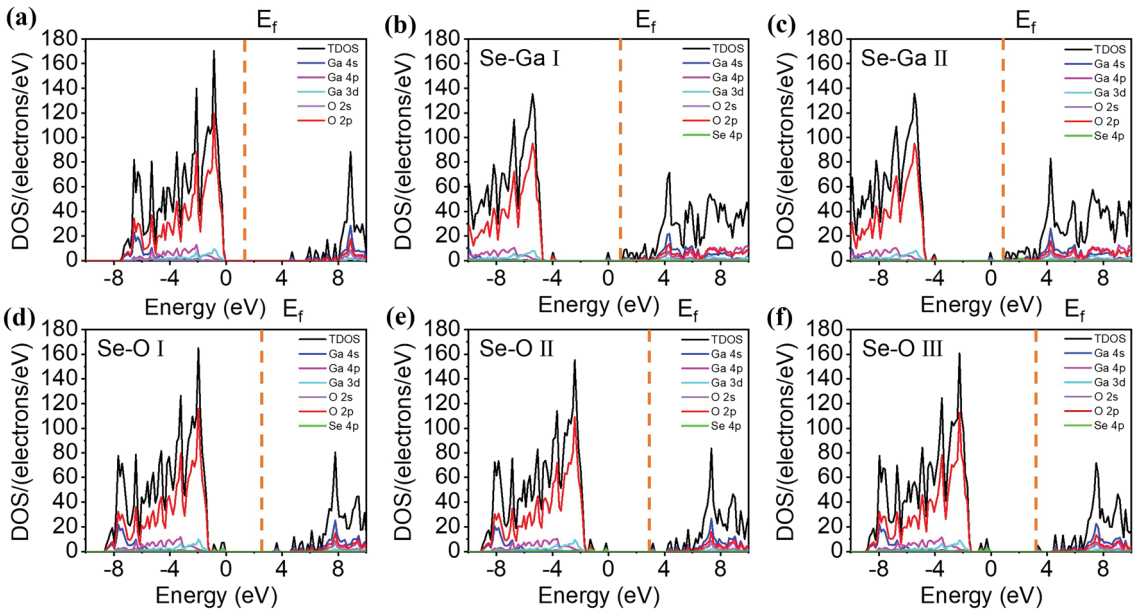

Fig. 5 Projected density of states of (a) pure β-Ga_2O_3 supercell, selenium doping at (b) Ga I, (c) Ga II, (d) O I, (e) O II, and (f) O III sites.

of β-Ga_2O_3. Additionally, considering the potential limitations of first-principles calculations can guide the design of targeted experimental studies to complement and validate the computational predictions. In the future, experimental studies will be conducted to validate theoretical calculations, explore different concentrations of selenium doping, and investigate combinations of dopants to achieve the desired properties. The discovery that selenium can replace oxygen or gallium under different conditions provides important guidance for future research. It is crucial to study the effects of different selenium doping concentrations on material properties, with the goal of improving electrical conductivity or enhancing optical characteristics. Additionally, combining selenium with other elements could yield valuable insights and lead to the creation of materials tailored for specific applications. These findings will guide future experimental work, including exploring various doping concentrations, element combinations, and validation methods. This approach has the potential to drive the development of advanced materials suitable for diverse applications.

Conclusion

In summary, the doping of β-Ga_2O_3 with selenium was investigated using DFT calculations, in which Se was found to exhibit the ability to incorporate both Ga and O sites under specified conditions. Specifically, selenium is more likely to substitute the Ga sites under O-rich conditions and is more likely to substitute the O sites under Ga-rich conditions. Interestingly, selenium acts as a shallow donor when it substitutes on Ga sites, implying the potential for achieving n-type conductivity in β-Ga_2O_3. However, it is expected that there will be no effect in tuning the conductivity of β-Ga_2O_3 if selenium substitutes on O sites, which can be attributed to the formation of an isoelectronic trap. Based on our present analysis, the doping of Se in β-Ga_2O_3 may represent a viable route towards achieving electrical conductivity tuning of β-Ga_2O_3 materials for electronic and optoelectronic device applications. This study differs from previous work by focusing on the doping of β-Ga_2O_3 with selenium and its effects on electrical conductivity using DFT calculations. This approach provides valuable insights into the potential of selenium doping in β-Ga_2O_3 for achieving electrical conductivity.

Supplementary Information The online version contains supplementary material available at https://doi.org/10.1007/s11664-024-11292-6.

Acknowledgments The work was supported by C. K. Tan start-up fund from the Hong Kong University of Science and Technology (Guangzhou), the State Administration of Foreign Experts Affairs China (No. QN2022030022L), and the Guangzhou Municipal Science and Technology Project (Nos. 2023A03J0003, 2023A03J0013, and 2023A04J0310). We thank Zhigao Xie (software support), Yinmin Liao (data curation support) and Yan Wang (methodology support). We gratefully acknowledge HZWTECH for providing the computation facility.

Conflict of interest The authors declare that they have no conflict of interest.

References

1. J. Zhang, P. Dong, K. Dang, Y. Zhang, Q. Yan, H. Xiang, J. Su, Z. Liu, M. Si, J. Gao, M. Kong, H. Zhou, and Y. Hao, Ultra-wide Bandgap Semiconductor Ga_2O_3 Power Diodes. *Nat. Commun.* 13, 3900 (2022).
2. Y. Qin, Z. Wang, K. Sasaki, J. Ye, and Y. Zhang, Recent Progress of Ga_2O_3 Power Technology: Large-Area Devices, Packaging and Applications. *Jpn. J. Appl. Phy.* 62, SF0801 (2023).
3. X. Ji, C. Lu, Z. Yan, L. Shan, X. Yan, J. Wang, J. Yue, X. Qi, Z. Liu, W. Tang, and P. Li, A Review of Gallium Oxide-based Power Schottky Barrier Diodes. *J. Phys. D Appl. Phys.* 55, 443002 (2022).
4. R. Chen, D. Wang, B. Feng, H. Zhu, X. Han, J. Ma, H. Xiao, and C. Luan, High Responsivity Self-Powered DUV Photodetectors based on β-Ga_2O_3/GaN Heterogeneous PN Junctions. *Vacuum* 215, 112332 (2023).
5. Z.X. Jiang, Z.Y. Wu, C.C. Ma, J.N. Deng, H. Zhang, Y. Xu, J.D. Ye, Z.L. Fang, G.Q. Zhang, J.Y. Kang, and T.Y. Zhang, P-type β-Ga_2O_3 Metal-Semiconductor-Metal Solar-Blind Photodetectors with Extremely High Responsivity and Gain-Bandwidth Product. *Mater. Today Phys.* 14, 100226 (2020).
6. M. Akatsuka, Y. Kawaguchi, R. Itoh, A. Ozawa, M. Yamamoto, T. Tanabe, and T. Yoshida, Preparation of Ga_2O_3 Photocatalyst Highly Active for CO_2 Reduction with Water Without Cocatalyst. *Appl. Catal. B* 262, 118247 (2020).
7. R. Roy, V.G. Hill, and E.F. Osborn, Polymorphism of Ga_2O_3 and the System Ga_2O_3-H_2O. *J. Am. Chem. Soc.* 74, 719 (2002).
8. M. Higashiwaki, K. Sasaki, A. Kuramata, T. Masui, and S. Yamakoshi, Development of Gallium Oxide Power Devices. *Phys. Status Solidi (A)* 211, 21 (2014).
9. J. Xu, W. Zheng, and F. Huang, Gallium Oxide Solar-Blind Ultraviolet Photodetectors: A Review. *J. Mater. Chem. C* 7, 8753 (2019).
10. A. Kuramata, K. Koshi, S. Watanabe, Y. Yamaoka, T. Masui, and S. Yamakoshi, High-Quality β-Ga_2O_3 Single Crystals Grown by Edge-Defined Film-Fed Growth. *Jpn. J. Appl. Phys.* 55, 1202A2 (2016).
11. X. Liu, C. Sammarco, G. Zeng, D. Guo, W. Tang, and C.-K. Tan, Investigations of Monoclinic- and Orthorhombic-based $(B_xGa_{1-x})_2O_3$ Alloys. *Appl. Phys. Lett.* 117, 012104 (2020).
12. X. Liu, and C.-K. Tan, Electronic Properties of Monoclinic $(In_xGa_{1-x})_2O_3$ Alloys by First-Principle. *AIP Adv.* 9, 035318 (2019).
13. J.B. Varley, A. Perron, V. Lordi, D. Wickramaratne, and J.L. Lyons, Prospects for n-type Doping of $(Al_xGa_{1-x})_2O_3$ Alloys. *Appl. Phys. Lett.* 116, 172104 (2020).
14. X. Liu, and C.-K. Tan, First-Principle Investigation of Monoclinic $(Al_xIn_yGa_{1-x-y})_2O_3$ Quaternary Alloys. *Semicond. Sci. Technol.* 35, 025023 (2020).
15. J. Cao, Z. Xie, Y. Wang, H. Song, G. Zeng, W. Tang, and C.-K. Tan, Fracture Toughness and Critical Thickness of β-$(In_xGa_{1-x})_2O_3$/Ga_2O_3 by First Principles. *J. Mater. Chem. C* 12, 1843 (2024).
16. M. Higashiwaki, β-Ga_2O_3 Material Properties, Growth Technologies, and Devices: A Review. *AAPPS Bull.* 32, 3 (2022).
17. J.B. Varley, J.R. Weber, A. Janotti, and C.G. Van de Walle, Oxygen Vacancies and Donor Impurities in β-Ga_2O_3. *Appl. Phys. Lett.* 97, 142106 (2010).
18. M. Yu, B. Peng, K. Sun, J. Yu, L. Yuan, J. Hu, Y. Zhang, and R. Jia, First Principles Investigation of Photoelectric Properties of Ga_2O_3 Doped with Group IV Elements (Si, Ge, Sn). *Mater. Today Commun.* 34, 105127 (2023).
19. A. Shokri, Y. Melikhov, Y. Syryanyy, and I.N. Demchenko, Point Defects in Silicon-Doped β-Ga_2O_3: Hybrid-DFT Calculations. *ACS Omega* 8, 43732 (2023).
20. Y.K. Frodason, P.P. Krzyzaniak, L. Vines, J.B. Varley, C.G. Van de Walle, and K.M.H. Johansen, Diffusion of Sn Donors in β-Ga_2O_3. *APL Mater.* 11, 041121 (2023).
21. H. Peelaers, and C.G. Van de Walle, Doping of Ga_2O_3 with Transition Metals. *Phys. Rev. B* 94, 195203 (2016).
22. J.L. Lyons, A Survey of Acceptor Dopants for β-Ga_2O_3. *Semicond. Sci. Technol.* 33, 05LT02 (2018).
23. C. Zhang, Z. Li, and W. Wang, Critical Thermodynamic Conditions for the Formation of p-type β-Ga_2O_3 with Cu Doping. *Materials* 14, 5161 (2021).
24. M.H. Wong, K. Sasaki, A. Kuramata, S. Yamakoshi, and M. Higashiwaki, Anomalous Fe Diffusion in Si-Ion-Implanted β-Ga_2O_3 and Its Suppression in Ga_2O_3 Transistor Structures Through Highly Resistive Buffer Layers. *Appl. Phys. Lett.* 106, 032105 (2015).
25. A. Luchechko, V. Vasyltsiv, L. Kostyk, O. Tsvetkova, and B. Pavlyk, The Effect of Cr^{3+} and Mg^{2+} Impurities on Thermoluminescence and Deep Traps in β-Ga_2O_3 Crystals. *ECS J. Solid State Sci. Technol.* 9, 045008 (2020).
26. X. Wang, R. Quhe, Y. Zhi, Z. Liu, Y. Huang, X. Dai, Y. Tang, Z. Wu, and W. Tang, The Electronic Structure and Magnetic Property of the Mn Doped β-Ga_2O_3. *Superlattices Microstruct.* 125, 330 (2019).
27. X.-Y. Yang, S.-M. Wen, D.-D. Chen, T. Li, and C.-W. Zhao, First-Principles Study of the Influence of Nb Doping on the Electronic Structure and Optoelectronic Properties of β-Ga_2O_3. *Phys. Lett. A* 433, 128025 (2022).
28. Z. Chen, D. Guo, P. Li, Z. Chen, W. Tang, and Q. Guo, Low Driven Voltage Red LEDs using Eu-Doped Ga_2O_3 Films on GaAs. *Appl. Phys. Express* 12, 061009 (2019).
29. K. Sawada, and T. Nakamura, Dynamics of Resonance Energy Transfer Process from Tb^{3+} to Eu^{3+} in Ga_2O_3 Phosphor. *J. Lumin.* 215, 116616 (2019).
30. Z. Chen, K. Saito, T. Tanaka, and Q. Guo, Near-Infrared Light-Emitting Diodes based on Tm-Doped Ga_2O_3. *J. Lumin.* 245, 118773 (2022).
31. L. Chen, K. He, G. Bai, H. Xie, X. Yang, and S. Xu, Non-contact Luminescence Thermometer based on Upconversion Emissions from Er^{3+}-Doped Beta-Ga_2O_3 with Wide Bandgap. *J. Alloys Compd.* 846, 156425 (2020).
32. X. Liu, and C.-K. Tan, Structural and Electronic Properties of Dilute-Selenide Gallium Oxide. *AIP Adv.* 9, 125204 (2019).
33. R. Bai, B. Zhao, K. Ling, K. Li, and X. Liu, Dilute-Selenium Alloying: A Possible Perspective for Achieving p-type Conductivity of β-Gallium Oxide. *J. Alloys Compd.* 891, 161969 (2022).
34. G. Kresse, and J. Furthmüller, Efficient Iterative Schemes Forab Initiototal-Energy Calculations using a Plane-Wave Basis Set. *Phys. Rev. B* 54, 11169 (1996).
35. P.E. Blöchl, Projector Augmented-Wave Method. *Phys. Rev. B* 50, 17953 (1994).
36. G. Kresse, and D. Joubert, From Ultrasoft Pseudopotentials to the Projector Augmented-Wave Method. *Phys. Rev. B* 59, 1758 (1999).
37. J.P. Perdew, K. Burke, and M. Ernzerhof, Generalized Gradient Approximation Made Simple. *Phys. Rev. Lett.* 77, 3865 (1996).
38. J. Heyd, G.E. Scuseria, and M. Ernzerhof, Hybrid Functionals based on a Screened Coulomb Potential. *J. Chem. Phys.* 118, 8207 (2003).
39. M. Orita, H. Ohta, M. Hirano, and H. Hosono, Deep-Ultraviolet Transparent Conductive β-Ga_2O_3 Thin Films. *Appl. Phys. Lett.* 77, 4166 (2000).

40. M. Huang, Z. Zheng, Z. Dai, X. Guo, S. Wang, L. Jiang, J. Wei, and S. Chen, DASP: Defect and Dopant Ab-initio Simulation Package. *J. Semicond.* 43, 042101 (2022).
41. C. Freysoldt, B. Grabowski, T. Hickel, J. Neugebauer, G. Kresse, A. Janotti, and C.G. Van de Walle, First-Principles Calculations for Point Defects in Solids. *Rev. Mod. Phys.* 86, 253 (2014).
42. C. Freysoldt, J. Neugebauer, and C.G. Van de Walle, Electrostatic Interactions between Charged Defects in Supercells. *Phys. Status Solidi (B)* 248, 1067 (2011).
43. C. Freysoldt, J. Neugebauer, and C.G. Van de Walle, Fully Ab Initio Finite-Size Corrections for Charged-Defect Supercell Calculations. *Phys. Rev. Lett.* 102, 016402 (2009).
44. S. Geller, Crystal Structure of β-Ga_2O_3. *J. Chem. Phys.* 33, 676 (1960).
45. T. Matsumoto, M. Aoki, A. Kinoshita, and T. Aono, Absorption and Reflection of Vapor Grown Single Crystal Platelets of β-Ga_2O_3. *Jpn. J. Appl. Phys.* 13, 1578 (1974).
46. A. Baldereschi, Theory of Isoelectronic Traps. *J. Lumin.* 7, 79 (1973).